Inorg. Chem. **1999,** *38,* 2143−2149 **2143**

Kinetic and Mechanistic Aspects of Sulfur Recovery from $Pd_2I_2(\mu\text{-}S)(\mu\text{-dpm})_2$ Using I_2 and Structures of Pd(II) Complexes with the Chelated Monosulfide of dpm[†]

Terrance Y. H. Wong, Steven J. Rettig, and Brian R. James*

Department of Chemistry, University of British Columbia, Vancouver,
British Columbia V6T 1Z1, Canada

Received August 27, 1998

The $Pd_2X_2(\mu\text{-}S)(dpm)_2$ complexes (**2**) (X = I, Br) react with halogens to yield $PdX_2(dpm)$ (**3**) and elemental sulfur. Kinetic and mechanistic studies on the X = I system in $CHCl_3$ reveal that the reaction proceeds via addition of I_2 to give $Pd_2I_4(dpm)_2$ (**4c**), which then undergoes unimolecular decomposition to generate $PdI_2(dpm)$ (**3c**); the liberated sulfur concatenates to form elemental S_8. The addition reaction is in the stopped-flow time regime and is first-order in both **2c** and I_2, with $\Delta H^\ddagger = 32 \pm 1$ kJ mol^{-1} and $\Delta S^\ddagger = -91 \pm 3$ J K^{-1} mol^{-1}. The slower decomposition reaction of **4c** is first order in **4c**, with $\Delta H^\ddagger = 80 \pm 1$ kJ mol^{-1} and $\Delta S^\ddagger = -26 \pm 3$ J K^{-1} mol^{-1}. Byproduct $PdX_2(dpm(S))$ (**5**) [dpm(S) = $Ph_2PCH_2P(S)Ph_2$] also forms under some conditions via reaction of **3** with an S_n species ($n < 8$). Complexes **5** (X = Cl (**a**), Br (**b**), I (**c**)) were also synthesized directly, and the structure of the **5c** species, as well as of $[Pd(dpm(S))_2]Cl_2$, were determined by X-ray analyses that reveal the envelope configuration of the five-membered $\overline{\text{Pd-PPh}_2\text{CH}_2\text{P(S)}}\text{Ph}_2$ chelate ring.

Introduction

The catalyzed conversion of H_2S to H_2 and elemental sulfur is a commercially attractive reaction,[1,2] and efforts have been undertaken in this laboratory to develop catalytic systems after our discovery of the solution reaction 1,[2−4] where X = halogen

$$Pd_2X_2(dpm)_2\ (\mathbf{1}) + H_2S \rightarrow Pd_2X_2(\mu\text{-}S)(dpm)_2\ (\mathbf{2}) + H_2 \quad (1)$$

(with **a**, **b**, and **c** referring to X = Cl, Br, and I, respectively) and dpm = bis(diphenylphosphino)methane. The bridged-S can be removed in "coordinated forms" from **2** completely or partially in solution using O-atom donors, CO, CN^-, biphenyl, butadiene or phosphines,[2,5,6] including dpm itself, which gives complete removal as dpm(S) and leads to the first reported homogeneously catalyzed conversion of H_2S to H_2 (eqs 2 and 3).[1]

$$Pd_2X_2(\mu\text{-}S)(dpm)_2\ (\mathbf{2}) + dpm \rightarrow Pd_2X_2(dpm)_2\ (\mathbf{1}) + dpm(S) \quad (2)$$

$$H_2S + dpm \rightarrow H_2 + dpm(S) \quad (3)$$

$$Pd_2X_2(\mu\text{-}S)(dpm)_2\ (\mathbf{2}) + X_2 \rightarrow 2\ PdX_2(dpm)\ (\mathbf{3}) + {}^{1}/_{8}S_8 \quad (4)$$

We have noted[1,2] that **2** also reacts with halogens when the sulfur is removed as elemental S_8 (eq 4) and the mononuclear, chelated dpm species is formed. The present paper reports on kinetic and mechanistic studies of reaction 4 for the X = I system; also reported are a side reaction and related diversions into the generation of coordinated dpm(S) ($Ph_2PCH_2P(S)Ph_2$). We have reported recently on the conversion of **3** to **2** by reaction with H_2S in the presence of γ-alumina (eq 5)[8] and, of

$$2\ PdX_2(dpm)\ (\mathbf{3}) + H_2S \rightarrow Pd_2X_2(\mu\text{-}S)(dpm)_2\ (\mathbf{2}) + 2\ HX \quad (5)$$

note, a combination of reactions 4 and 5, coupled with the known photodecomposition of HI to generate H_2 and I_2, leads to the net reaction $H_2S \rightarrow H_2 + {}^{1}/_{8}S_8$. We show here that reaction 4 proceeds via transannular addition to form the tetrahalodipalladium(II) intermediate $Pd_2X_4(\mu\text{-dpm})_2$ (**4**), a species detected previously in the reaction between **1** and X_2.[7]

Experimental Section

The materials used, synthetic procedures for the ligands and complexes, and instrumentation used for ^1H and $^{31}P\{^1H\}$ NMR, ESR, and UV−vis spectra were described previously.[1,4,5] The mono- and disulfides (dpm(S),[1] dpm(S)$_2$[9]) and the complexes $PdCl_2(PhCN)_2$,[10] **1a**−**c**,[11] **2a**−**c**,[5] and **3a**,**b**[12,13] were synthesized using published methods. All experiments were performed under N_2 unless otherwise specified.

Kinetically fast reactions were monitored by stopped-flow measurements using a quartz cell path length of 1 cm on an Applied Photophysics stopped-flow spectrometer (Model SF.17MV) equipped with a 150 W xenon arc lamp, temperature-regulating unit, and the SF.17MV kinetic software. Mass spectrometric analyses were performed

---

[†] For convenience, μ-dpm (Bis(diphenylphosphino)methane) in all the dinuclear species is written simply as dpm.

(1) Wong, T. Y. H.; Barnabas, A. F.; Sallin, D.; James, B. R. *Inorg. Chem.* **1995**, *34*, 2278.

(2) James, B. R. *Pure Appl. Chem.* **1997**, *69*, 2213.

(3) Lee, C.-L.; Besenyei, G.; James, B. R.; Nelson, D. A.; Lilga, M. A. *J. Chem. Soc., Chem. Commun.* **1985**, 1175.

(4) Barnabas, A. F.; Sallin, D.; James, B. R. *Can. J. Chem.* **1989**, *64*, 2009.

(5) Besenyei, G.; Lee, C.-L.; Gulinski, J.; James, B. R.; Nelson, D. A.; Lilga, M. A. *Inorg. Chem.* **1987**, *26*, 3622.

(6) Weng, W. Z.; Sallin, D.; James, B. R. To be published.

(7) Hunt, C. T.; Balch, A. L. *Inorg. Chem.* **1981**, *20*, 2267.

(8) Wong, T. Y. H.; James, B. R.; Wong, P. C.; Mitchell, K. A. R. *J. Mol. Catal. A: Chem.* **1999**, *139*, 159.

(9) Carmalt, C. J.; Cowley, A. H.; Decken, A.; Lawson, Y. G.; Norman, N. C. *Acta Crystallogr.* **1996**, *C52*, 931.

(10) Doyle, J. R.; Slade, P. E.; Jonassen, H. B. *Inorg. Synth.* **1960**, *6*, 216.

(11) Balch, A. L.; Benner, L. S. *Inorg. Synth.* **1982**, *21*, 47.

(12) Jenkins, J. M.; Verkade, J. G. *Inorg. Synth.* **1968**, *11*, 108.

(13) Steffen, W. L.; Palenik, G. J. *Inorg. Chem.* **1976**, *15*, 2432.

10.1021/ic981039w CCC: $18.00

using a Kratos MS50 spectrometer (EI) operating at 150 °C with an electron energy of 70 eV. Infrared spectra (KBr pellet) were recorded using an ATI Mattson Genesis Series FTIR spectrometer.

PdI_2(dpm) (3c). To $PdCl_2$(dpm) (0.10 g, 0.18 mmol) in CH_2Cl_2 (20 mL) at room temperature (rt) was added a solution of NaI (0.40 g, 2.7 mmol) in aqueous MeOH (10 mL). The resulting orange solution was stirred for 1 h before being reduced in volume under vacuum to ~10 mL. Et_2O (30 mL) was added to precipitate an orange solid that was filtered off, washed successively with aqueous MeOH (2 × 10 mL) and Et_2O (10 mL), and dried in vacuo. Yield: 0.13 g (97%). ^{1}H NMR (20 °C, $CDCl_3$): δ 7.0−8.0 m (20H, Ph), δ 4.42 t (2H, CH_2, J_{PH} = 10.0 Hz). $^{31}P\{^1H\}$ NMR (20 °C, $CDCl_3$): δ −63.2 s. UV−vis (20 °C, $CHCl_3$) λ, nm (ϵ, M^{-1} cm^{-1}): 430 (6455). Anal. Calcd for $C_{25}H_{22}I_2P_2$-Pd: C, 40.33; H, 2.98. Found: C, 40.34; H, 2.97.

PdX_2(dpm(S)) (5). $PdCl_2(PhCN)_2$ (0.10 g, 0.26 mmol) and dpm(S) (0.11 g, 0.26 mmol) were dissolved in CH_2Cl_2 (20 mL), and the resulting solution was stirred at rt for 1 h before the volume was reduced to ~10 mL to precipitate completely $PdCl_2$(dpm(S)) (**5a**). The solid was filtered off, washed with Et_2O (2 × 10 mL), and dried in vacuo (yield 0.15 g (97%)). $PdBr_2$(dpm(S)) (**5b**) and PdI_2(dpm(S)) (**5c**) were prepared from a CH_2Cl_2 solution (20 mL) of **5a** (0.10 g, 0.17 mmol) via halide exchange with $^nPr_4NBr$ (0.67 g, 2.52 mmol) or $^nBu_4NI$ (0.93 g, 2.52 mmol), respectively, dissolved in CH_2Cl_2 (5 mL). The procedures then followed those for **5a**. Yield: **5b**, 0.11 g (96%); **5c**, 0.13 g (97%). Anal. Calcd for $C_{25}H_{22}Cl_2P_2PdS$ (**5a**): C, 50.57; H, 3.73. Found: C, 50.56; H, 3.74. Anal. Calcd for $C_{25}H_{22}Br_2P_2PdS$ (**5b**)·CH_2Cl_2: C, 40.68; H, 3.15. Found: C, 41.23; H, 3.11. Anal. Calcd for $C_{25}H_{22}I_2P_2PdS$ (**5c**)·0.5CH_2Cl_2: C, 37.39; H, 2.83. Found: C, 36.88; H, 2.73. UV−vis: **5a**, λ 372 (1500); **5b** λ 396 (2180), 374 sh (2095); **5c** λ 478 (3000), 420 sh (1735). Crystals of **5a** and **5c** for X-ray crystallographic analysis were grown at rt via diffusion of hexanes (10 mL) or Et_2O (10 mL) into a 6 mL CH_2Cl_2 solution of 10 mg of the respective compound. For **5a**, the crystals were not of sufficiently good quality for a satisfactory X-ray crystallographic analysis, although the essential square plane coordination geometry was delineated.

$PdCl_2(dpm(S)_2)$. $PdCl_2(PhCN)_2$ (0.10 g, 0.26 mmol) and $dpm(S)_2$ (0.12 g, 0.26 mmol) were stirred in CH_2Cl_2 (10 mL) at rt, the solution color changing from yellow to orange with accompanying precipitation of an orange-red solid. The mixture was stirred for 1 h before Et_2O (20 mL) was added to complete the precipitation. The solid was filtered off, washed with Et_2O (2 × 10 mL), and dried in vacuo; (yield 0.13 g (80%)). This compound is not thermally stable, and attempts to dry it at 40 °C result in decomposition as evidenced by NMR. Furthermore, the compound has limited solubility in CH_2Cl_2 and $CHCl_3$ but is soluble in DMSO. ^{1}H NMR (20 °C, DMSO-d_6): δ 7.0−8.0 (20H, Ph), δ 5.54 t (2H, CH_2, J_{PH} = 14 Hz). $^{31}P\{^1H\}$ NMR (20 °C, DMSO-d_6): δ 37.3 s. UV−vis (20 °C, CH_2Cl_2): λ 418 (1.0), 322 (13.5) (relative intensities).

$[Pd(dpm(S))_2]Cl_2$. To dpm(S) (0.27 g, 0.65 mmol) dissolved in 5 mL of CH_2Cl_2 was added a solution of $PdCl_2(PhCN)_2$ (0.050 g, 0.15 mmol) in 5 mL of CH_2Cl_2. The resulting orange-red solution was stirred at rt for 1 h and then reduced in volume to ~5 mL. Et_2O (20 mL) was then added to precipitate an orange solid that was filtered off, washed with Et_2O (2 × 10 mL), and dried in vacuo (yield 0.12 g (91%)). ^{1}H NMR (20 °C, DMSO-d_6): δ 7.0−8.0 m (40H, Ph), δ 5.66 pt (4H, CH_2). $^{31}P\{^1H\}$ NMR (20 °C, DMSO-d_6): δ 49.6, 37.6 (AB pattern, J_{PP} = 23 Hz). A yellow crystal, obtained by diffusion of hexanes (10 mL) into a CH_2Cl_2 (6 mL) solution of 10 mg of the complex, was analyzed by X-ray crystallography.

$Pd_2I_2(\mu$-SO)$(dpm)_2$. The synthesis follows that used previously for the analogous chloro complex.[5] To $Pd_2I_2(\mu$-S)$(dpm)_2$ (0.20 g, 0.16 mmol) dissolved in CH_2Cl_2 (10 mL) was added H_2O_2 (1 mL of a 30% aqueous solution in 5 mL MeOH). The color immediately changed from brown to red-brown. The solution was stirred for 1 h before MeOH (25 mL) was added to precipitate a red-brown solid that was filtered off, washed with MeOH (2 × 10 mL), and dried in vacuo. Yield: 0.16 g (80%). ^{1}H NMR (20 °C, $CDCl_3$): δ 7.0−8.0 m (40H, Ph), δ 4.98 d t (1H, CH_2, J_{HH} = 12 Hz, J_{PH} = 13.5 Hz), δ 4.18 d t (1H, CH_2, J_{HH} = 15 Hz, J_{PH} = 9 Hz), δ 2.58 m (1H, CH_2), δ 2.26 m (1H, CH_2). $^{31}P\{^1H\}$ NMR (20 °C, $CDCl_3$): δ 19 to −7, a broadened AA′BB′ pattern. ν(SO) = 979 cm^{-1}. A satisfactory elemental analysis could not be obtained.

X-ray Crystallographic Analyses. PdI_2(dpm(S))(5c)·0.5CH_2Cl_2. A single crystal having approximate dimensions of 0.05 × 0.20 × 0.30 mm was mounted in a glass capillary. All intensity measurements were made on a Rigaku AFC6S diffractometer with graphite-monochromated Mo Kα radiation (λ = 0.710 69 Å). Cell constants along with orientation matrixes were obtained from a least-squares refinement of the setting angles of 25 reflections in the range $14.2 < 2\theta < 24.7°$. Intensity data were collected at 21 °C using the $\omega - 2\theta$ scan technique. The intensities of three representative reflections were measured after every 200 reflections, and no decay correction was applied. The data were corrected for Lorentz and polarization effects. The structure was solved by direct methods[14] and expanded using Fourier techniques.[15] The CH_2Cl_2 solvent is disordered about a center of symmetry—the disorder was modeled by a single 0.5 occupancy carbon atom and three partially occupied Cl sites. The solvent C atom and two of the Cl atoms were refined with isotropic thermal parameters. Hydrogen atoms associated with the metal complex were fixed in calculated positions with C−H = 0.98 Å. Neutral atom scattering factors[16] and anomalous dispersion terms[17] were taken from the usual sources. All calculations were performed using teXsan.[18]

$[Pd(dpm(S))_2]Cl_2·2CH_2Cl_2$. A single crystal having approximate dimensions of 0.15 × 0.25 × 0.35 mm was analyzed in a manner similar to that described above for PdI_2(dpm(S)); 25 reflections in the range $27.8 < 2\theta < 32.9°$ were used for the unit cell determination. The structure analysis was initiated in the centrosymmetric space group $P\bar{1}$, this choice being validated by subsequent calculations. The cation has exact inversion symmetry, and there are two molecules of CH_2Cl_2 per complex cation.

Kinetic Studies. The kinetics of the decomposition of the intermediate $Pd_2I_4(dpm)_2$ (**4c**) in reaction 4 for X = I in $CHCl_3$ were monitored at 20−35 °C by conventional spectrophotometric measurements at 396 nm in a thermostated 1 cm quartz cell (volume 1.5 mL), after a 0.050 mL solution of I_2 ($[I_2] = (3.8-7.5) \times 10^{-4}$ M) was injected into a 1.00 mL solution of **2c** ($[\mathbf{2c}] = (1.6-9.9) \times 10^{-5}$ M). Pseudo-first-order conditions were maintained, standard log(absorbance difference) vs time plots gave excellent linearity for at least 2.5−3 half-lives, and corresponding rate constants, k_{obs}, were evaluated from the semilog plots or calculated directly by fit of the data using the kinetic software. Some kinetic measurements in CH_2Cl_2 and MeCN were conducted at 24.0 °C using $[\mathbf{2c}] = 9.4 \times 10^{-5}$ M and $[I_2] = 7.5 \times 10^{-4}$ or 9.4×10^{-5} M, respectively, the absorbance changes being monitored at 396 and 360 nm, respectively.

The kinetics of the formation of **4c** in $CHCl_3$ (and a single experiment in CH_2Cl_2) were measured spectrophotometrically using a stopped-flow apparatus. Two thermostated 1-mL loading syringes were filled with solutions of the appropriate concentrations of **2c** and I_2, respectively. Absorbance changes were conveniently monitored at 510 nm (in $CHCl_3$) or 530 nm (in CH_2Cl_2), which are isosbestic points with respect to decomposition of **4c**. Pseudo-first-order rate constants, k'_{obs}, were determined from the average of four replicate experiments using a standard nonlinear regression, algorithmic fitting equation.

Mechanistic Studies

(a) NMR Scale. The S-Abstraction Reaction. This reaction (**2c** → **3c**, eq 4) in $CDCl_3$ (or CD_3CN) for varying **2c**:1 ratios was monitored at rt using ^{1}H and $^{31}P\{^1H\}$ NMR. Variable-temperature NMR experiments also were performed at −42 to +80 °C under vacuum or aerobic conditions in an NMR tube

---

(14) SIR92: Altomare, A.; Burla, M. C.; Camalli, M.; Cascarano, M.; Giacovazzo, C.; Guagliardi, A.; Polidori, G. *J. Appl. Crystallogr.*, in preparation.

(15) DIRDIF92: Beurskens, P. T.; Admiraal, G.; Beurskens, G.; Bosman, W. P.; Garcia-Granda, S.; Gould, R. O.; Smits, J. M. M.; Smykall, C. *The DIFDIF program system, Technical Report of the Crystallography Laboratory*, University of Nijmegen, The Netherlands.

(16) Cromer, D. T.; Waber, J. T. *International Tables for X-ray Crystallography*; The Kynoch Press: Birmingham, England, 1974; Vol. 4, Table 2.2A.

(17) Ibers, J. A.; Hamilton, W. C. *Acta Crystallogr.* **1964**, *17*, 781.

(18) teXsan: Crystal Structure Analysis Package, Molecular Structure Corp., 1985, 1992.

Table 1. NMR Data for the Palladium Complexes **3a**−**c**, **4a**−**c**, and **5a**−**c**[a]

compound	δ, ^{1}H[b]	δ, ^{31}P{^{1}H}
$PdCl_2$(dpm) (**3a**)	4.21 t (10.8)	−54.7
$PdBr_2$(dpm) (**3b**)	4.37 t (10.5)	−56.2
PdI_2(dpm) (**3c**)	4.42 t (10.0)	−63.2
	4.74 t (10.0)[c]	−55.7[c]
$Pd_2Cl_4(dpm)_2$ (**4a**)	4.55 qn (4.6)[d]	8.5[d]
$Pd_2Br_4(dpm)_2$ (**4b**)	4.6 br s[d]	4.90[d]
$Pd_2I_4(dpm)_2$ (**4c**)	5.14 qn (3.7)[e]	−1.52
	5.18 qn (4.0)[d]	−0.73[d]
	5.08 qn (3.9)[c]	1.54[c]
$PdCl_2$(dpm(S)) (**5a**)	4.07[f]	54.9, 30.9 (18.3)[g]
$PdBr_2$(dpm(S)) (**5b**)	4.02[f]	56.6, 32.1 (20.4)[g]
PdI_2(dpm(S)) (**5c**)	3.71[f]	61.1, 31.3 (25.5)[g]

[a] Unless stated otherwise, data in $CDCl_3$ (for **3**, **5**) or CD_2Cl_2 (for **4**) at 20 °C with respect to TMS or 85% H_3PO_4; J_{HH}, J_{PH}, and/or J_{PP} values in Hz are given in parentheses. [b] Signals for CH_2 protons. [c] In CD_3CN. [d] Taken from ref 7. [e] In $CDCl_3$. [f] Pseudotriplet. [g] AB pattern.

fitted with a J. Young valve (Aldrich), the solvent (~0.5 mL $CDCl_3$) being vacuum transferred onto solid **2c** and I_2 using liquid N_2. Samples, prepared by simultaneous injection of equimolar solutions of **2c** and I_2 into NMR or ESR tubes held at low temperatures, were also studied. Other solvents (acetone, MeOH, C_6H_6, CCl_4, dimethylacetamide, DMF, EtOAc, and toluene) tested were found unsuitable because of insolubility of **2c** or formation of charge-transfer adducts with I_2. The X = Br system (**2b** → **3b**) was briefly examined at rt in $CDCl_3$, the Br_2 being added to a solution of **2b** via vacuum transfer. TLC studies of the NMR samples were carried out using $CHCl_3$ eluent to analyze for elemental sulfur.

Other Reactions of Complexes with Elemental Sulfur or I_2. Reactions of sulfur with **1c**, **2c**, and **3c** were examined in $CDCl_3$, under thermal (20−90 °C) or photolytic conditions (450 W Hg lamp at 20 °C); an in situ sample of **4c** (formed at −42 °C by a 1:1 reaction of **1c** with I_2) was also tested for reactivity toward sulfur. Finally, a reaction of $Pd_2I_2(\mu\text{-SO})(dpm)_2$ with I_2 in $CDCl_3$ at rt was monitored by NMR and TLC.

(b) Synthetic Scale. Schlenk techniques were employed; for example, the iodo complex **2c** (0.050 g, 0.039 mmol) was reacted with I_2 (0.010 g, 0.039 mmol) in $CHCl_3$ (20 mL), and the reaction was monitored by UV−vis spectroscopy. After 24 h, the supernatant red liquid was decanted off, leaving a pale yellow solid (S_8) that was washed with acetone (2 × 10 mL) and dried in vacuo (yield: ~1 mg) prior to analysis. Solvent removal from the supernatant yielded the red-orange solid (**3c**).

Results

Complexes $Pd_2X_2(dpm)_2$ (**1**), $Pd_2X_2(\mu\text{-S})(dpm)_2$ (**2**), and PdX_2(dpm) (**3**) have been generally well-characterized previously.[1,5,11−13] NMR spectroscopic data for **1** and **2** have been tabulated elsewhere;[1] those for **3**, $Pd_2X_4(dpm)_2$ (**4**), and PdX_2(dpm(S)) (**5**) are given in Table 1, while those for $PdCl_2$(dpm(S)$_2$) and $Pd_2I_2(\mu\text{-SO})(dpm)_2$ are given in the Experimental Section.

An NMR study of the reaction 4 (X = I) revealed, in general, a well-behaved system (Figure 1); the formation of small amounts of PdI_2(dpm(S)) (**5c**) will be discussed later. Addition of a purple I_2 solution to an equimolar brown solution of **2c** leads to consumption of the reactants with concomitant formation of a green-black intermediate species (**4c**) and its subsequent decomposition to the orange-red product **3c**; **4c**, which can be generated also from reaction of $Pd_2I_2(dpm)_2$ (**1c**) with I_2,[7] is characterized as $Pd_2I_4(dpm)_2$ by the NMR data (Table 1). The final solution (after 1 h) contained a small amount of a yellow solid (~0.1 mg), identified by TLC as elemental sulfur. A corresponding synthetic-scale reaction of **2c** and I_2 behaved similarly and after ~3 h yielded ~1 mg of S_8 (characterized by TLC, UV−vis (in Et_2O), MS (EI), and its reaction with $Pd_2I_2(dpm)_2$ (**1c**) which gave only **2c**).[19]

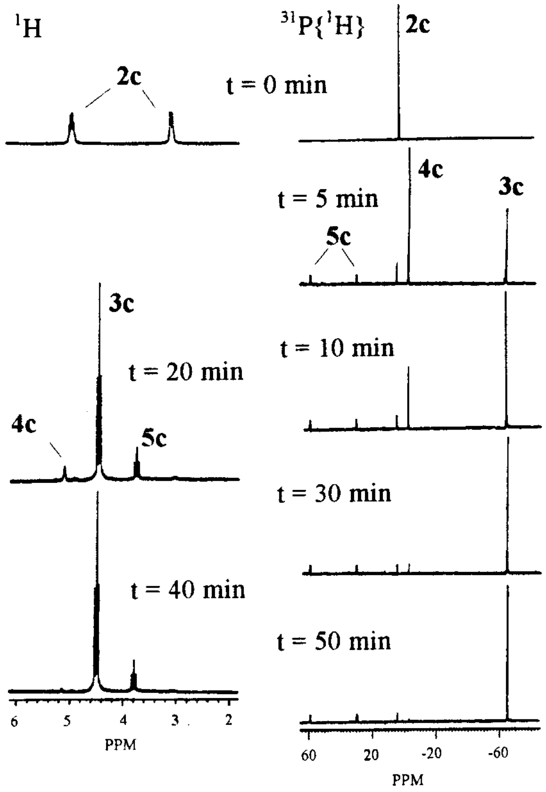

Figure 1. ^{1}H (300 MHz) and ^{31}P{^{1}H} (121 MHz) NMR study of the reaction of $Pd_2I_2(dpm)_2$ (**2c**, 1.6 × 10^{-2} M) with 1 mol equiv of I_2 in $CDCl_3$ at rt: **3c** = PdI_2(dpm), **4c** = $Pd_2I_4(dpm)_2$, **5c** = PdI_2(dpm(S)).

Kinetic Studies. In $CHCl_3$, **2c** is brown (λ_{max} = 368 and 485 nm), while **3c** is orange (λ_{max} = 429 nm). Figure S1 (Supporting Information) illustrates spectral changes on treatment of **2c** with I_2 with a corresponding first-order rate-plot shown in the inset; the "immediate" spectrum (t = 30 s, dashed line) shows a λ_{max} at 362 nm with a shoulder at 484 nm. Below 420 and above 484 nm, the absorbance rapidly decreases while simultaneously increasing in the region between; the next spectrum recorded (t = 150 s) corresponds to the intermediate **4c** essentially fully formed and now decomposing to **3c**. The spectral changes accompanying this decomposition are characterized by two isosbestic points at 420 and 510 nm. Optical density was monitored at 396 nm where I_2 and S_8 have no absorptivities. The pseudo-first-order rate constants, k_{obs}, were independent of both [I_2] and [**2c**]. The rate law for the conversion of **4c** to **3c** may thus be defined by k_D:

$$\text{rate} = -\frac{d[\mathrm{Pd_2I_4(dpm)_2}\ (\mathbf{4c})]}{dt} = k_{obs}[\mathbf{4c}] = k_D[\mathbf{4c}]$$

The temperature dependence data for k_D (Table 2) gave an excellently linear Eyring plot with $\Delta H_D^{\ddagger} = 80 \pm 1$ kJ mol^{-1} and $\Delta S_D^{\ddagger} = -26 \pm 3$ J mol^{-1} K^{-1}.

For the stopped-flow time scale reaction between **2c** and I_2 to form the intermediate **4c**, inspection of data from the conventional UV−vis measurements (Figure S1, Supporting

---

(19) Balch, A. L.; Benner, L. S.; Olmstead, M. M. *Inorg. Chem.* **1979**, *18*, 2996.

Table 2. Rate Constants for the Bimolecular Formation (k_I) and Unimolecular Decomposition (k_D) of $Pd_2I_4(dpm)_2$(**4c**)[a]

T, K	k_I, $M^{-1}\ s^{-1}$	k_D, $\times 10^{-3}\ s^{-1}$
292.6	179	2.2
297.0	1389[b]	0.65[b] (0.69)[b,c] (3.6)[c]
298.0	235 (240)[d]	4.0
303.1	290	7.8
308.2	370	13.1

[a] In $CHCl_3$, unless otherwise stated. [b] In CH_2Cl_2. [c] Measured following formation of **4c** by the reaction of I_2 with $Pd_2I_2(dpm)_2$. [d] Five-fold excess of $^nBu_4NI$ present.

Information) led to the choice of 510 nm to monitor the fast reaction, as the decrease in absorbance here ceased with complete formation of **4c** because isosbesticity was then observed during its decomposition. The observed pseudo-first-order rate constants, k'_{obs}, were first-order with respect to I_2 and independent of [**2c**] (Figures S2 and S3, Supporting Information). Thus, the rate law is defined by:

$$\text{rate} = -\frac{d[\mathbf{2c}]}{dt} = k'_{obs}[\mathbf{2c}] = k_I[I_2][\mathbf{2c}]$$

Values of k_I (Table 2) give an excellent Eyring plot and $\Delta H_I^{\ddagger} = 32 \pm 1$ kJ mol^{-1} and $\Delta S_I^{\ddagger} = -91 \pm 3$ J mol^{-1} K^{-1}. No kinetic role for I^- was found, in that addition of excess $^nBu_4NI$ had little effect on k_I (Table 2). Using the $\Delta H_I^{\ddagger}$ and $\Delta S_I^{\ddagger}$ values, k_I at −42 °C is calculated to be ~4.1 M^{-1} s^{-1} with a corresponding $t_{1/2}$ of ~15 s for second-order conditions when $[Pd_2] = [I_2] = 0.016$ M. This correlates well with the low-temperature NMR studies where **4c** was observed to be completely formed under such conditions in ~3 min.

Studies of reaction 4 (X = Br) in $CHCl_3$ were complicated by reaction of Br_2 with the solvent,[20] which occurs over the same time scale as the reaction between **2b** and Br_2 (as evidenced by UV−vis studies). Nevertheless, in a 1:1 reaction for 24 h at rt, about half of **2b** had been consumed to generate **3b** and **5b** in a 2:1 ratio along with S_8.

Attempts to study solvent effects on the reaction of **2c** with I_2 were generally thwarted by reactivity of I_2 toward the solvent. Of the several systems studied (see the Experimental Section), some NMR data were obtained in CD_3CN; a 1:1 reaction at rt immediately generated quantitatively **4c**, which then decomposed in minutes to give **3c** and **5c** (~2:1), and S_8 was detected. In MeCN, the presence of excess I_2 led to rapid decomposition of **3c**, and this limited the use of UV−vis for kinetic studies. Nevertheless, a study of a 1:1 reaction at rt revealed data similar to those of Figure S1 (Supporting Information) with a λ_{max} at 360 nm attributed to **4c** and generation of an isosbestic point at 414 nm during its subsequent decomposition. The studies were again complicated by accompanying reaction of I_2 with the solvent. A few kinetic experiments were carried out in CH_2Cl_2 (Table 2).

Formation of $PdX_2(dpm(S))$, X = I (5c) and Br (5b). The "spurious" resonances detected in the NMR studies of reaction 4, X = I (Figure 1), were shown to result from the presence of the byproduct **5c** that was subsequently synthesized independently using dpm(S). The structure of **5c** (see below) reveals coordination via P- and S-atoms, and the solution NMR data are consistent with this. In NMR-scale experiments (with **2c**/I_2 = 1 or 2) at rt to 80 °C under anaerobic or aerobic conditions, **5c** was formed in 15−25% yield (of total Pd); in synthetic-scale reactions, **5c** formed to an extent of 5%, while in the UV−vis studies **5c** was not detected (after a workup procedure). The yield of recovered S in NMR- and synthetic-scale studies of reaction 4, X = I, was typically ~80%. In an NMR-scale reaction at rt using I_2/**2c** = 2, no **5c** was seen during complete formation of **3c**, and also *no free S_8 was detected*. At −42 °C (NMR scale), when the $Pd_2I_4(dpm)_2$ intermediate **4c** was fully formed within a few minutes, no **5c** was detected; when the temperature was raised slowly to ~20 °C, decomposition of **4c** to $PdI_2(dpm)$ (**3c**) was observed, but again **5c** was not seen. With use of such a "warming-up" procedure, **5c** was never generated. When equimolar $CDCl_3$ solutions of **2c** and I_2 (1:1) at rt were injected into an NMR tube at −78 or −42 °C, trace amounts (<1%) of **5c** and **3c** were seen; there were no subsequent changes in the −78 °C sample, while at −42 °C, **4c** was formed with the trace amounts of **5c** and **3c** remaining unchanged. Related studies using ESR tubes were carried out in attempts to detect S_n radicals (e.g., n = 1, 2), but no ESR signals were seen.

Table 3. Crystallographic Data for $PdI_2(dpm(S))$ (**5c**)·$0.5CH_2Cl_2$ and $[Pd(dpm(S))_2]Cl_2 \cdot 2CH_2Cl_2$

formula	$C_{25.50}H_{23}ClI_2P_2PdS$	$C_{52}H_{48}Cl_6P_4PdS_2$
fw	819.13	1180.08
space group	$P2_1/n$ (#14)	$P\bar{1}$ (#2)
a/Å	9.378(2)	11.612(1)
b/Å	14.231(3)	11.813(1)
c/Å	21.049(2)	10.3623(7)
α/deg		97.898(6)
β/deg	91.60(1)	96.011(7)
γ/deg		80.174(8)
V/Å	2808.1(9)	1382.4(2)
Z	4	1
ρ_c/(g cm^{-3})	1.937	1.417
T/°C	21	21
λ/Å	0.710 69	0.710 69
μ(Mo Kα)/cm^{-1}	31.57	8.50
R^a	0.035	0.036
$R_w{}^b$	0.028	0.033

[a] $R = \sum||F_o| - |F_c||/\sum|F_o|$. [b] $R_w = (\sum w(|F_o| - |F_c|)^2/\sum wF_o^2)^{-1/2}$, $w = 1/\sigma^2(F_o)$.

Reaction of $Pd_2I_2(\mu\text{-SO})(dpm)_2$ with I_2 (1:1) at rt generated (together with S_8) 35% of **5c** and 65% of **3c** with complete loss of the μ-SO reactant.

Reaction of $Pd_2I_2(dpm)_2$ (**1c**) with S_8 in $CDCl_3$ at rt after 24 h gave only $Pd_2I_2(\mu\text{-S})(dpm)_2$ (**2c**). Under purely thermal conditions, S_8 showed no reactivity toward **3c**, but use of photolytic conditions (Hg lamp) gave complete conversion to **5c**. At −42 °C, the stable **4c** was unreactive toward 1 mol equiv of S_8, and when the temperature was raised to rt no **5c** accompanied the formation of **3c**.

Crystal Structures. Crystal data, information relating to data collection, refinement details, and selected bond distances and angles for **5c** (as $PdI_2(dpm(S))\cdot 0.5CH_2Cl_2$) and $[Pd(dpm(S))_2]Cl_2$ are given in Tables 3 and 4, and the molecular structures are shown in Figures 2 and 3, respectively. A complete table of crystallographic data, final atomic coordinates and equivalent isotropic thermal parameters, anisotropic thermal parameters, bond lengths, bond angles, torsion angles, intermolecular contacts, and least-squares planes for both structures is included as Supplementary Information.

In **5c**, the Pd atom is in an approximately square-planar coordination environment, but there is slight tetrahedral distortion with I(1) and P(1) lying slightly above the plane [0.0079(7) and 0.075(2) Å, respectively] and I(2) and S slightly below the plane [0.0085(7) and 0.084(2) Å, respectively]. The Ph_2PCH_2P-

---

(20) Streitwieser, A., Jr.; Heathcock, C. H. *Introduction to Organic Chemistry*, 3rd ed.; Macmillan: New York, 1985; Chapter 6.

Table 4. Selected Bond Lengths (Å) and Angles (deg) for $PdI_2(dpm(S))$ (**5c**) and $[Pd(dpm(S))_2]Cl_2$

(a) Compound $PdI_2(dpm(S))$ (**5c**)			
I(1)−Pd(1)	2.6419(9)	I(2)−Pd(1)	2.6006(9)
Pd(1)−S(1)	2.331(2)	Pd(1)−P(1)	2.243(2)
S(1)−P(2)	2.007(3)	P(1)−C(1)	1.860(8)
P(1)−C(2)	1.815(8)	P(1)−C(8)	1.805(8)
P(2)−C(1)	1.814(8)	P(2)−C(14)	1.799(8)
P(2)−C(20)	1.802(8)		
I(1)−Pd(1)−I(2)	92.97(3)	I(1)−Pd(1)−S(1)	86.28(6)
I(1)−Pd(1)−P(1)	177.90(7)	I(2)−Pd(1)−S(1)	177.64(6)
I(2)−Pd(1)−P(1)	87.14(6)	S(1)−Pd(1)−P(1)	93.69(8)
Pd(1)−S(1)−P(2)	101.3(1)	Pd(1)−P(1)−C(1)	109.0(3)
Pd(1)−P(1)−C(2)	116.9(3)	Pd(1)−P(1)−C(8)	115.0(3)
C(1)−P(1)−C(2)	102.9(4)	C(1)−P(1)−C(8)	103.3(4)
C(2)−P(1)−C(8)	108.3(4)	S(1)−P(2)−C(1)	106.3(3)
S(1)−P(2)−C(14)	109.6(3)	S(1)−P(2)−C(20)	113.2(3)
C(1)−P(2)−C(14)	110.6(4)	C(1)−P(2)−C(20)	107.5(4)
C(14)−P(2)−C(20)	109.6(4)	P(1)−C(1)−P(2)	107.8(4)
P(1)−C(2)−C(3)	119.1(6)	P(1)−C(2)−C(7)	122.7(7)
(b) Compound $[Pd(dpm(S))_2]Cl_2$			
Pd(1)−S(1)	2.3256(8)	Pd(1)−P(1)	2.3229(7)
Cl(2)−C(26)	1.684(6)	Cl(3)−C(26)	1.654(7)
S(1)−P(2)	2.017(1)	P(1)−C(1)	1.835(3)
P(1)−C(2)	1.814(3)	P(1)−C(8)	1.809(3)
P(2)−C(1)	1.791(3)	P(2)−C(14)	1.791(3)
P(2)−C(20)	1.797(3)		
S(1)−Pd(1)−S(1)[a]	180.0	S(1)−Pd(1)−P(1)	91.21(3)
S(1)−Pd(1)−P(1)[a]	88.79(3)	P(1)−Pd(1)−P(1)[a]	180.0
Pd(1)−S(1)−P(2)	99.84(4)	Pd(1)−P(1)−C(1)	110.46(9)
Pd(1)−P(1)−C(2)	110.71(9)	Pd(1)−P(1)−C(8)	115.52(10)
C(1)−P(1)−C(2)	106.8(1)	C(1)−P(1)−C(8)	105.7(l)
C(2)−P(1)−C(8)	107.1(1)	S(1)−P(2)−C(1)	107.48(10)
S(1)−P(2)−C(14)	107.60(10)	S(1)−P(2)−C(20)	112.8(1)
C(1)−P(2)−C(14)	111.6(1)	C(1)−P(2)−C(20)	108.1(1)
C(14)−P(2)−C(20)	109.3(1)	P(1)−C(1)−P(2)	106.1(1)

[a] Symmetry operation: $1 - x, 1 - y, 1 - z$.

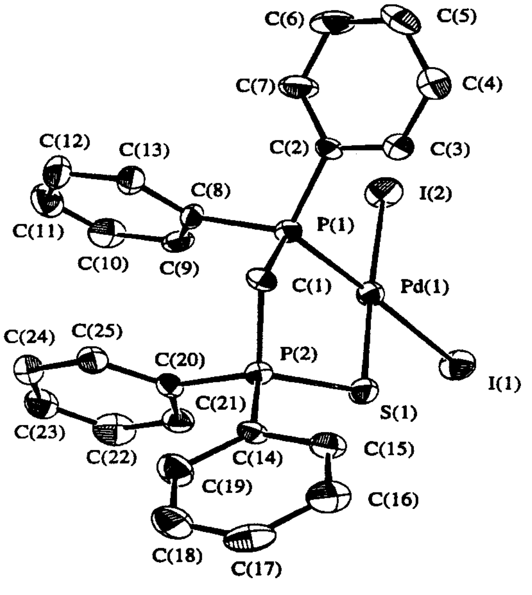

Figure 2. ORTEP drawing of $PdI_2(dpm(S))$ (**5c**); H-atoms omitted. 33% probability thermal ellipsoids are shown.

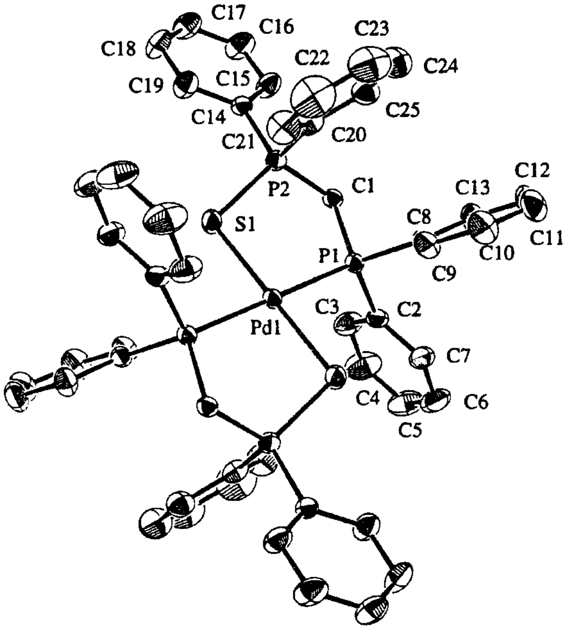

Figure 3. ORTEP drawing of $[Pd(dpm(S))_2]Cl_2$; H-atoms omitted. 33% probability thermal ellipsoids are shown.

$(S)Ph_2$ ligand, which coordinates via the P- and S-atoms within a five-membered chelate ring, lies in a twisted conformation so that P(2) is above the coordination plane, 0.698 Å, a so-called envelope configuration. The P(1)−C(1) and P(2)−C(1) bond distances and P(1)−C(1)−P(2) bond angle are within the normal ranges seen for P−C single bonds[21,22] and P−C−P angles,[22,23] and the P(2)−S and Pd−S bond distances are not unusual.[22−24] The Pd−I(1) bond distance trans to the Pd−P(1) bond is ~0.041 Å shorter than the Pd−I(2) bond distance trans to the Pd−S(1) bond, in keeping with the greater trans influence of P versus S.[24−26]

In $[Pd(dpm(S))_2]Cl_2$, the cation has exact inversion symmetry and the Pd has square-planar coordination. The two dpm(S) ligands coordinate via the P- and the S-atoms, again forming envelope chelate rings with the two P (and S)-atoms mutually trans. The chelate ligands lie in twisted conformations so that one P(2) atom is above and one is below the Pd−S(1)−P(1)-C(1) coordination planes (by 0.854 Å). The P(1)−C(1), P(2)−C(1), P(2)−S, and Pd−S bond distances and the P(1)−C(1)-P(2) bond angle are again normal. The two S−Pd−P(1) angles are 91.21(3) and 88.79(3)°.

Discussion

Reaction of **2c** with I_2 proceeds in two stages to yield **3c** and elemental S_8 (eq 6). Transannular addition via electrophilic

$$Pd_2I_2(\mu\text{-}S)(dpm)_2\ (\mathbf{2c}) + I_2 \xrightarrow[-\text{“S”}]{k_1} Pd_2I_4(dpm)_2\ (\mathbf{4c}) \xrightarrow{k_D} 2\ PdI_2(dpm)\ (\mathbf{3c}) \quad (6)$$

attack of I_2 occurs rapidly with quantitative formation of the intermediate **4c** and presumably monatomic sulfur. Thereafter, a slower unimolecular decomposition of **4c** generates **3c**, and concatenation of “S” leads to elemental S_8. An interesting side reaction generates small amounts of $PdI_2(dpm(S))$ (**5c**) (see below). Hunt and Balch have reported previously the reaction of $Pd_2I_2(dpm)_2$ (**1c**) with I_2, which also proceeds via **4c** to generate **3c**.[7]

---

(21) Corbridge, D. E. C. *The Structure Chemistry of Phosphorus*; Elsevier: Amsterdam, 1974; p 7.

(22) Baker, M. J.; Giles, M. F.; Orpen, A. G.; Taylor, M. J.; Watt, R. J. *J. Chem. Soc., Chem. Commun.* **1995**, 197.

(23) Berry, D. E.; Browning, J.; Dixon, K. R.; Hitts, R. W. *Can. J. Chem.* **1988**, *66*, 1272.

(24) Balakrishna, M. S.; Klein, R.; Uhlenbrock, S.; Pinkerton, A. A.; Cavell, R. G. *Inorg. Chem.* **1993**, *32*, 5676.

(25) Appleton, T. G.; Clark, H. C.; Manzer, L. E. *Coord. Chem. Rev.* **1973**, *10*, 335.

(26) Zumdahl, S. S.; Drago, R. S. *J. Am. Chem. Soc.* **1968**, *90*, 6669.

Formation of 4c. The k_I step is simply first-order in both **2c** and I_2, and the formation of **4c** is conveniently pictured as proceeding via a concerted process involving transition state **I**, akin to reactions involving addition of acetylenes across the Pd−Pd bond.[27] Subsequent electron flow through the metal centers results in the oxidation of the sulfide to "S" with concomitant reduction of I_2 to iodide. Alternatively, an initial electrophilic attack at one metal center is plausible. A transition state such as **II** would be generated that, following associative substitution, leads to **III** (with I^- perhaps not "fully formed" or free), and subsequent nucleophilic attack of I^- at the second Pd center, perhaps via transition state **IV**, would finally give **4c**. There is ample precedence for the involvement of ionic intermediates in halogen-addition reactions across metal centers.[28−30]

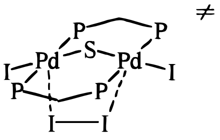

I

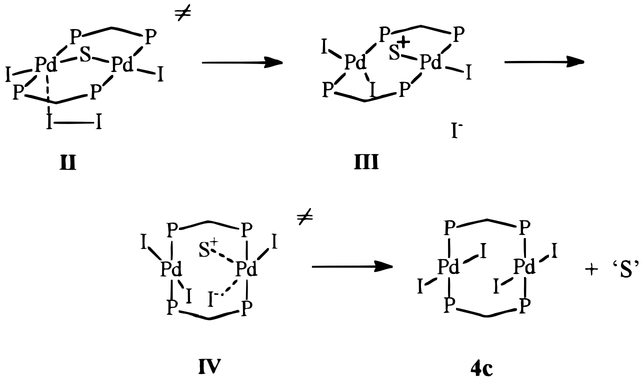

The rate for the process outlined in eq 7, assuming a steady-state treatment for **III**, is ($k_1k_2/(k_{-1} + k_2)$)[**2c**][I_2], which is also consistent with the experimental findings, including the independence of the rate on added I^-. Of note, the accelerated rates

$$Pd_2I_2(\mu\text{-}S)(dpm)_2 + I_2 \underset{k_{-1}}{\overset{k_1}{\rightleftharpoons}} \mathbf{III} + I^- \xrightarrow{k_2} Pd_2I_4(dpm)_2 + \text{“S”} \qquad (7)$$

in the more polar CH_2Cl_2[29] (by a factor of ~6 (Table 2)) and MeCN (where the formation of **4c** was now too fast for investigation by stopped-flow) also tend to favor an ionic pathway.

The activation parameters $\Delta H_I^\ddagger = 32$ kJ mol^{-1} and $\Delta S_I^\ddagger = -91$ J mol^{-1} K^{-1} are typical of those seen for addition at either one or two metal centers[4,27,31,32] and are comparable to values reported for halogenation of the complexes $M_2(CO)_8L_2$ (M = Mn, Re; L = $Me_2AsC{=}C(AsMe_2)CF_2CF_2$, $Ph_2PC{=}C(PPh_2)CF_2CF_2$), reactions for which ionic halide intermediates were favored.[30]

To our knowledge, there is only one other report describing addition of a halogen to a "sulfide" complex with concomitant formation of S_8 (eq 8), but no kinetic or mechanistic data were reported.[33]

$$Os(\eta^2\text{-}S_2)(CO)_2(PPh_3)_2 + I_2 \rightarrow OsI_2(CO)_2(PPh_3)_2 + {}^1/{}_4S_8 \qquad (8)$$

Kinetic studies of the reaction of **2b** with Br_2 were attempted in the present study, but reactivity of Br_2 with the solvent (replacement of $H^\bullet$ by $Br^\bullet$)[20] interfered with reproducibility of the results. A qualitative NMR study, however, revealed that the X = Br system reacts faster than the X = I system. In other reactions involving halogens, greater reactivity of Br_2 has been attributed to it being a less "selective electrophile" than I_2, as reflected in proceeding through a less ordered transition state than with I_2 (i.e., $\Delta S^\ddagger$ is less negative for Br_2 systems).[29] Solvent iodination does not occur,[34] and I-atoms are unlikely to have a role in reaction 6 as this takes place in the absence of light and/or at low temperatures.

Decomposition of 4c. The findings for the k_D step (eq 6) complement quantitatively those of Hunt and Balch on the reaction of **1** with I_2;[7] for the decomposition of **4c** in CD_2Cl_2 at 15 °C, they reported $t_{1/2} = 360$ s (from NMR data). Our $t_{1/2}$ value in CH_2Cl_2 at 24 °C is ~1000 s. The data for k_D in $CHCl_3$ at 25 °C and CH_2Cl_2 at 24 °C (Table 2) show a faster rate by ~6 in the less polar $CHCl_3$, consistent with nonionic pathways. We have also determined comparable k_D values following formation of **4c** by reaction of **1c** with I_2 (Table 2).

Decomposition of **4c** may be envisaged as proceeding via transition state **V**:[7]

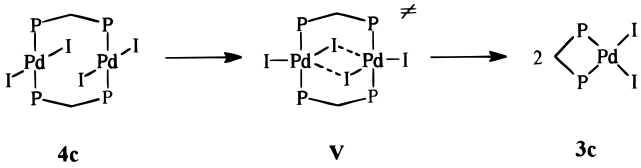

The activation parameters, $\Delta H_D^\ddagger = 80$ kJ mol^{-1} and $\Delta S_D^\ddagger = -26$ J mol^{-1} K^{-1}, obtained in the present study, could be consistent with such a mechanism. The small negative entropy change could reflect the unimolecular rearrangement of **4c** to **V**, while the relatively large enthalpy term could reflect the energy required to overcome the proximity and strain effects in forming the halide bridges. Alternatively, some degree of Pd−P bond breaking could be important in the transition state. Kinetic data for the decompositions of $Pd_2Br_4(dpm)_2$ (**4b**) and $Pd_2Cl_4(dpm)_2$ (**4a**) are not yet available. Of note, **4a** and **4b** are also observed as the low-temperature products in the reactions of **1a** and **1b** with 2 mol equiv of HCl and HBr, respectively (eq 9).[2,35]

---

(27) Xie, L. Y.; James, B. R. *Inorg. Chim. Acta* **1994**, *217*, 209.

(28) Haines, R. J.; du Preez, A. L. *J. Chem. Soc. A* **1970**, 2341 and references therein.

(29) Chipperfield, J. R.; Ford, J.; Hayter, A. C.; Lee, D. J.; Webster, D. E. *J. Chem. Soc., Dalton Trans.* **1976**, 1024 and references therein.

(30) Cullen, W. R.; Hou, F. L. *Inorg. Chem.* **1975**, *14*, 312

(31) Brost, R. D.; Fjeldsted, D. O. K.; Stobbart, S. R. *J. Chem. Soc., Chem. Commun.* **1989**, 488.

(32) (a) Atwood, J. D. *Inorganic and Organometallic Reaction Mechanisms*; Brooks/Cole: New York, 1985; Chapter 5. (b) Collman, J. P.; Hegedus, L. S.; Norton, J. R.; Finke, R. G. *Principles and Applications of Organotransition Metal Chemistry*; University Science Books: Mill Valley, CA, 1987; Chapter 5.

(33) Farrar, D. H.; Grundy, K. R.; Payne, N. C.; Roper, W. R.; Walker, A. *J. Am. Chem. Soc.* **1979**, *101*, 6577.

(34) Meislich, H.; Nechamkin, H.; Sharefkin, J. *Theory and Problems of Organic Chemistry*, 2nd ed.; McGraw-Hill: Toronto, 1991; Chapter 4, p 57.

(35) Barnabas, A. F. M. Sc. Dissertation, University of British Columbia, Vancouver, 1989.

$$Pd_2X_2(dpm)_2\ (\mathbf{1}) \xrightarrow{HX} [XPd(H)(dpm)_2PdX_2] \xrightarrow[-H_2]{HX} Pd_2X_4(dpm)_2\ (\mathbf{4}) \quad (9)$$

Formation of $PdI_2(dpm(S))$ (5c). Depending on experimental conditions, the byproduct **5c** is formed, and the yield of S_8 in the overall reaction (eqs 4 and 6) is affected. Qualitative evidence, as summarized below, suggests that the yield of **5c** results from competition of two reactions, concatenation to form S_8, perhaps via S_1[36] (eq 10) (although no paramagnetic species were detected by ESR), and the reaction of an S_n species ($n < 8$) with **3c** (eq 11).

$$S_n + S \rightarrow S_{n+1} \quad (10)$$

$$S_n + PdI_2(dpm)\ (\mathbf{3c}) \rightarrow PdI_2(dpm(S))\ (\mathbf{5c}) + S_{n-1} \quad (11)$$

As S_8 is unreactive toward **2c**, **3c** (under thermal conditions), and **4c**, an assumed S_n species, shown to be unreactive toward **2c** and **4c**, is implicated in the reaction with **3c** to form **5c**, and strong support for this suggestion comes from the observed reaction of S_8 with **3c** under photolytic conditions (eq 12), which presumably occurs via initial ring opening of S_8.[37]

$$PdI_2(dpm) + {}^{1}/_{8}S_8 \xrightarrow[\sim 1\ \text{day}]{h\nu} PdI_2(dpm(S)) \quad (12)$$

The yields of **5c** can be rationalized semiquantitatively in terms of rates of reactions 10 and 11.[38] Interestingly, in the reaction of $Pd_2I_2(\mu\text{-}SO)(dpm)_2$ with I_2, the increased yield of **5c** probably results from the slower decomposition of free SO species (which gives elemental S_8 and dioxygen),[39a] and in the reaction of **2c** with excess I_2, the absence of both **5c** and S_8 is attributed to scavenging by I_2 for an S_n species to form the known iodosulfanes S_nI_2, where $n \geq 2$[39b] (I_2 exhibits no reactivity with **5c** or with S_8).

Formation of $PdI_2(dpm(S)_2)$ is not observed; the energetics perhaps favor formation of the five-membered Pd(P−S) ring in **5c**, where the axial phenyl groups are seen to be positioned away from one another (Figure 3), as opposed to a six-membered Pd(S−S) ring that might invoke axial phenyl group interactions. An independent synthesis of $PdCl_2(dpm(S)_2)$ was attempted, but its identity has not been unequivocally established; however, the $^{31}P\{^1H\}$ singlet at δ 37.3 is consistent with the presence of Pd−S═P moieties (cf. data for $PdCl_2(dpm(S))$ (**5a**) and $[Pd(dpm(S))_2]Cl_2$). Transition-metal complexes containing chelating $dpm(S)_2$, as well as $dpm(Se)_2$, are known.[40−43] Complex **5a** was readily synthesized from $PdCl_2(PhCN)_2$ and 1 mol equiv of dpm(S), with **5b** and **5c** being synthesized via subsequent halide metathesis reactions.

The structure of **5c** (as the $0.5CH_2Cl_2$ solvate), completed here in January 1994, was among the first for a chelated dpm(S) system; that of RhCl(CO)(dpm(S)),[22] which contains the same "envelope"-type five-membered chelate ring, appeared in 1995. The structurally characterized $PtCl(PEt_3)(R_2PCH_2P(S)R_2)$[23] and $M(cod)(R_2PCH_2P(S)R_2)$ ($M = Rh, Ir$; $R = {}^tBu$)[44] also contain the (P−S) chelated ring, while $RuCl_2$(*p*-cymene)((dpm(S)) contains the dpm(S) ligand bonded only via the P-atom;[44] corresponding complexes containing $R_2PCH_2P(Se)R_2$ ($R = Ph$, ^tBu) have been isolated but not characterized structurally.[23,44]

Reaction of excess dpm(S) with $PdCl_2(PhCN)_2$ generates the bis-chelated species $[Pd(dpm(S))_2]Cl_2$, one of the first structurally characterized bis-dpm(S) complexes; the coordinated PPh_2 moieties are found to be mutually trans, possibly because a cis arrangement would give rise to unfavorable steric interactions between the phenyls. However, both *cis*- and *trans*-$[Pt(dpm(S))_2]^{2+}$ species have been postulated to exist in solution on the basis of NMR data,[45] and an X-ray structure of *trans*-$[RhCl_2(dpm(S))_2]PF_6$ reveals mutually *cis*-PPh_2 groups.[46]

Acknowledgment. We thank the Natural Sciences and Engineering Council of Canada for a research grant (B.R.J.) and the University of British Columbia for a Graduate Fellowship (T.Y.H.W.). Johnson Matthey Ltd. kindly provided some of the palladium as $PdCl_2$.

Supporting Information Available: Tables of crystallographic data, atomic coordinates and equivalent isotropic thermal parameters, anisotropic thermal parameters, complete bond lengths and angles, torsion angles, intermolecular contacts, and least-squares planes for the structures of **5c**·0.5 CH_2Cl_2 and $[Pd(dpm(S))_2]Cl_2 \cdot 2CH_2Cl_2$ and Figures S1−S3. This material is available free of charge via the Internet at http://pubs.acs.org.

IC981039W

---

(36) Williams, C. R.; Harpp, D. N. *Sulfur Lett.* **1993**, *16*, 63.
(37) Giannotti, C.; Ducourant, A. M.; Chanaud, H.; Chiaroni, A.; Riche, C. *J. Organomet. Chem.* **1977**, *140*, 289 and references therein.
(38) Wong, T. Y. H. Ph.D. Dissertation, University of British Columbia, Vancouver, 1996.
(39) (a) Meyer, B.; Jensen, D.; Oommen, T. In *Sulfur in Organic and Inorganic Chemistry*; Senning, A., Ed.; Marcel Dekker: New York, 1972; Vol. 2, Chapter 12. (b) Johnson, D. A. In *Sulfur in Organic and Inorganic Chemistry*; Senning, A., Ed.; Marcel Dekker: New York, 1972; Vol. 2, Chapter 13.
(40) Gimano, M. C.; Jones, P. G.; Laguna, A.; Sarroca, C. *J. Chem. Soc., Dalton Trans.* **1998**, 1277.
(41) Bond, A. M.; Colton, R.; Ebner, J.; Ellis, S. R. *Inorg. Chem.* **1989**, *28*, 4509 and references therein.
(42) Peringer, P.; Schwald, J. *J. Chem. Soc., Chem. Commun.* **1986**, 1625.
(43) Ainscough, E. W.; Bergen, H. A.; Brodie, A. M.; Brown, K. A. *J. Chem. Soc., Dalton Trans.* **1976**, 1649.
(44) Browning, J.; Bushnell, G. W.; Dixon. K. R.; Hilts, R. W. *J. Organomet. Chem.* **1993**, *452*, 205.
(45) Colton, R.; Ebner, J.; Hoskins, B. F. *Inorg. Chem.* **1988**, *27*, 1993.
(46) Abu-Gnim, C.; Rettig, S. J.; James, B. R. To be published.